Chemical Geology 668 (2024) 122351

Contents lists available at ScienceDirect

Chemical Geology

journal homepage: www.elsevier.com/locate/chemgeo

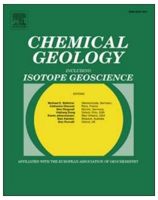

Testing triple oxygen isotope preservation in the new OPEnS totalizer against conventional monthly rainfall collectors

L. Nicole Arellano [a,*], Emily J. Beverly [a,b], John S. Selker [c], Mitchell Nelke [c], Gurpreet Singh [c], Cara Walter [c]

[a] Department of Earth and Atmospheric Sciences, University of Houston, Science and Research Building 1 Room 214, 3507 Cullen Blvd, Houston, TX 77204, USA
[b] Department of Earth and Environmental Science, University of Minnesota – Twin Cities, 116 Church Street SE, Minneapolis, MN 55455, USA
[c] Department of Biological and Ecological Engineering, Oregon State University, 116 Gilmore Hall, Corvallis, OR 97331, USA

ARTICLE INFO

Editor: Dr. Christian France-Lanord

Keywords:
Monthly precipitation
Rainfall totalizer
Water evaporation
Isotopic fractionation
d-excess
$\Delta'^{17}O$

ABSTRACT

Understanding the mechanisms that drive spatial and temporal triple oxygen isotope ($\Delta'^{17}O$) variations in modern precipitation is the first step to expanding the utility of these measurements as an environmental tracer jointly with traditional stable isotope parameters δD, $\delta^{18}O$, and d-excess. However, “totalizers” designed to collect a single precipitation sample pooled over a calendar month and minimize evaporation and associated isotopic fractionation of the sample during that time have not been tested for $\Delta'^{17}O$. We conducted a 30-day laboratory experiment comparing mass losses and isotopic shifts in four totalizers: 1) the OPEnS (Openly Published Environmental Sensing) totalizer, 2) the classic oil-based totalizer, 3) the commercial tube dip-in/pressure equilibration totalizer (Palmex Ltd. RS1), and 4) a reference totalizer (the control, lacking any evaporation reduction mechanism). The OPEnS totalizer was designed as being readily user built with parts costs of about $10, oil-free to facilitate quick and easy sample preparation and risk-free sample analysis, and its collection device expands as it fills to maintain a small gas/water ratio and minimize internal evaporative losses. All totalizers were filled to 12 % of their 3-L volume and placed in a modified laboratory oven with a diurnal temperature change of 23 to 40 °C and an average relative humidity of 9.1 % to simulate extreme evaporative conditions. The OPEnS totalizer experienced the smallest mass loss of water (0.21 %) and smallest isotopic shifts ($p < 0.05$ for $\delta^{18}O$ and d-excess), which were all within measurement error. The oil, tube, and reference totalizers showed larger mass losses (0.41, 1.37, and 1.61 %, respectively) and evaporative enrichment with respect to δD (+0.3, +0.8, and + 2.1 ‰), $\delta^{18}O$ (+0.16, +0.23, and + 0.83 ‰), and d-excess (−0.9, −1.0, and − 4.5 ‰). The $\Delta'^{17}O$ variations for all totalizers were within measurement error, so we suggest that in less harsh climates their triple oxygen isotope changes during secondary evaporation would be more acceptable. To test the OPEnS totalizer in field settings, we installed it alongside oil totalizers to collect monthly precipitation over three years in the towns of Jolly and San Antonio, Texas, with mean annual precipitation, temperature, and windspeed values of 556 and 563 mm, 18.7 and 21.9 °C, and 5.0 and 3.5 m/s, respectively. Results indicate that the OPEnS and oil totalizers can produce similar isotopic data in the field, but modifications to OPEnS have been implemented to minimize under-catch and stabilize the collection component where high winds are present and additional testing under a variety of environmental conditions is ongoing. OPEnS is scalable according to expected monthly precipitation amounts, providing a cost-effective, high-performance device for quantification of total rainfall and its isotopic composition without oil contamination risks.

1. Introduction

Various rainfall collectors have been developed for studies that utilize hydrogen and/or oxygen isotopes in water as natural tracers. For studies requiring frequent (daily, event-based, or intra-event-based) sample collection, such as those investigating storm events (Risi et al., 2010; Kaseke et al., 2018; Sánchez-Murillo et al., 2019; Sun et al., 2022) or set in hyper-arid environments that experience very few precipitation

---

* Corresponding author.
E-mail addresses: lnarella@central.uh.edu (L.N. Arellano), ebeverly@umn.edu (E.J. Beverly), john.selker@oregonstate.edu (J.S. Selker), nelkem@oregonstate.edu (M. Nelke), gurpreet.singh@oregonstate.edu (G. Singh), cara.walter@oregonstate.edu (C. Walter).

https://doi.org/10.1016/j.chemgeo.2024.122351
Received 26 March 2024; Received in revised form 14 August 2024; Accepted 23 August 2024

events each year (Wang et al., 2016; Zhu et al., 2021), standard rain gauges or sequential samplers are often appropriate. Sequential samplers collect samples of rainfall in temporal or volumetric intervals (Fischer et al., 2019). The implementation of these strategies long-term can be demanding and expensive, as they entail continuous staff observation and, in some instances, the use of highly sophisticated equipment. Up to hundreds of samples may be compiled, making analytical efforts costly as well. Alternatively in the case of prolonged studies, a cumulative, integrated monthly sampling strategy (e.g., a single sample pooled over a calendar month by a device referred to as a "totalizer") minimizes the time and costs needed for sample collection and is compliant with most monitoring networks worldwide (Kralik et al., 2004; Schürch et al., 2003; Stumpp et al., 2014; Vreča and Malenšek, 2016).

The Global Network of Isotopes in Precipitation (GNIP), initiated by the International Atomic Energy Agency (IAEA) and the World Meteorological Organization (WMO) in 1960, is a continuously expanding and publicly accessible monitoring network of δ^3H, δD (δ^2H), and δ^{18}O isotopes largely from monthly precipitation (IAEA and WMO, 2018). The technical guide that details sampling procedures for GNIP stations emphasizes the importance of avoiding secondary evaporation, or evaporation from totalizers after precipitation events have been collected throughout a cumulative sampling period, which would render the sample's isotopic data unrepresentative of the natural water cycle (IAEA, 2014). However, the risk of secondary evaporation is high using a monthly sampling strategy, especially at sites with hot, dry climates. Although comparative studies of different rain gauges have been conducted since 1955 (summarized by Sevruk et al., 2009), it was not until recently that Michelsen et al. (2018) conducted the first comprehensive comparison of monthly rainfall totalizer devices based on δD, δ^{18}O, and d-excess (deuterium-excess, $\delta D - 8 \times \delta^{18}O$; Dansgaard, 1964). To our knowledge, a similar comparison for triple oxygen isotopes, e.g., δ^{17}O and Δ'^{17}O (^{17}O-excess, $\ln(\delta^{17}O + 1) - 0.528 \times \ln(\delta^{18}O + 1)$; Barkan and Luz, 2007) is missing from the literature.

The recent development of high precision analytical methods (Barkan and Luz, 2005; Steig et al., 2014; Schauer et al., 2016) and demonstration of small variations in the relationship between δ^{17}O and δ^{18}O associated with different mass-dependent processes (Angert et al., 2004; Barkan and Luz, 2005, 2007) have shed light on the potential of Δ'^{17}O to provide additional information regarding evaporative regimes. Like d-excess, Δ'^{17}O is an indicator of evaporative fractionation controlled mainly by relative humidity at the site of evaporation and is visualized as a deviation from the Global Meteoric Water Line (GMWL) reference relationship (Fig. S1). The GMWLs for the oxygen-hydrogen and triple oxygen isotope systems have been calculated from large scale observations, and their slopes reflect equilibrium fractionation during condensation as the primary control on isotopic compositions of precipitation (Craig, 1961; Luz and Barkan, 2010). Any evaporation occurring during or after precipitation will result in kinetic fractionation, producing lines with slopes less than the GMWLs. The Δ'^{17}O parameter differs from the d-excess parameter in the following ways: (1) units are in per meg or parts per million (1 per meg = 0.001 per mille) and (2) it uses logarithmic forms of δ^{17}O and δ^{18}O, simplified in the literature by a prime symbol (e.g., δ'^{17}O and δ'^{18}O). Per meg units are necessary for expressing such small signal variability as exhibited by δ^{17}O and logarithmic notation is required to linearize the exponential relationship between δ^{17}O and δ^{18}O, thereby avoiding non-linear calculation artifacts that bias Δ'^{17}O (Barkan and Luz, 2007; Aron et al., 2021). Furthermore, isotopic fractionation associated with temperature changes between 10 and 45 °C alters Δ'^{17}O values less than measurement error (Barkan and Luz, 2005; Cao and Liu, 2011) but produces substantial d-excess variations between 0 and 20 °C (Majoube, 1971). Thus, the combination of traditional isotope parameters with Δ'^{17}O can help to disentangle the equilibrium and kinetic fractionation effects on isotopic compositions.

Given its small-signal variability and ability to uniquely track kinetic processes, it is imperative to quantify the variation in Δ'^{17}O associated with secondary evaporation during precipitation collection and storage using rainfall totalizers. Therefore, the first objective of this study is to consider if rainfall totalizers are appropriate for triple oxygen isotope studies by determining whether secondary evaporative shifts are within measurement error. Building on the work of Michelsen et al. (2018), who conducted an experiment using several totalizer designs to track the evaporative losses and δD, δ^{18}O, and d-excess shifts over 32 days under hot and dry conditions (temperatures of 26 to 45 °C, relative humidity less than 3 %), we tested the ability of totalizers to preserve triple oxygen isotope compositions in extreme environments. We focus our test on four totalizers: 1) the OPEnS (Openly Published Environmental Sensing) totalizer, 2) the classic oil-based totalizer, 3) the commercially available tube dip-in/pressure equilibration totalizer (Palmex Ltd. RS1; Gröning et al., 2012), and 4) a reference totalizer/the control, lacking any evaporation reduction mechanism (Fig. S2). OPEnS is a new totalizer that is readily user-built with parts costs of about \$10 and does not involve oil or internal headspace (see Section 2). No traditional or triple oxygen isotope data have been published using this new design. Therefore, the second objective of this study is to compare the shifts in δ^{18}O, δD, d-excess, and Δ'^{17}O over time associated with our new design to those associated with the well-established oil-based and tube dip-in totalizers.

2. Materials and methods

2.1. Tested totalizers

2.1.1. Conventional totalizers

The oil-based and tube dip-in totalizers performed best of the six totalizer designs tested in the Michelsen et al. (2018) study. Oil-based totalizers consist of a funnel connected to a collection bottle and rely on a layer of pure paraffin or silicone oil to isolate collected rainfall from the atmosphere. Before a sample can be taken the oil and water must be fully separated, as any oil fraction remaining in the water sample can severely compromise laboratory analyses by isotope ratio mass spectrometry (IRMS) or laser spectroscopy (Prechsl et al., 2014; Hartmann et al., 2018). Oil removal is a challenging process, and unsuccessful attempts may result in sample disposal (IAEA, 2014; Sánchez-Murillo et al., 2017). The tube dip-in sampler was designed to avoid any need of oil for evaporation prevention (Palmex Ltd. RS1; Gröning et al., 2012). Rather than cover the bottle's exposed water surface with oil, this design reduces the exposed surface to 0.3 % of its original area. This is done via a weighted plastic tube that extends from the funnel to the bottom of the bottle. After the first few millimeters of rain, the water level rises into the tube, so that only the small surface area of water inside the tube remains exposed to the atmosphere. Still, an additional plastic tube connects the bottle's headspace to outside air so that the air pressure inside the bottle remains on level with the outside atmospheric pressure. Otherwise, water could rise back up through the weighted tube into the funnel and evaporate. The relative volume and length of this tube allows only negligible moisture exchange between the bottle's headspace and the outside atmosphere; however, the bottle's headspace can be quite large and conducive to critical in-bottle evaporative losses when monthly precipitation amounts are low (Crawford et al., 2017). For our test, the reference totalizer consisted of the same funnel and bottle components as the oil-based totalizer but lacked an oil layer or any other evaporation reduction mechanism.

2.1.2. OPEnS totalizer

The OPEnS totalizer was designed and 3-D printed using stereolithography (SLA) to obtain a gas-tight product by the Openly Published Environmental Sensing (OPEnS) Lab at Oregon State University. The original OPEnS totalizer (version 1.0) was designed to attach to the METER Group ATMOS41 weather station and direct rain falling into the station's rain gauge into a collection bag via an inlet spout on the OPEnS totalizer that is secured to the rain gauge's water exit spout using cable ties or metal clamps (Fig. 1A). A spring inside of the weather station's rain gauge acts as a filter to keep out large debris, and the OPEnS totalizer has a removable cap to facilitate cleaning if needed. The bottom of the OPEnS totalizer 1.0 has screw threads for a 1000-mL Mylar foil collection bag (IMPAK Corporation FTSSP1000CSISL). Estimated costs for the 3-D printed OPEnS unit and 10 bags collection bags is ~$10. The 1000-mL bags have a 16 mm spout, but it is possible to use thread adapters to make the totalizer compatible with 3000-mL bags (IMPAK Corporation CSP0912BG04) in regions with high precipitation rates. These bags expand as they fill, maintaining a low gas/water ratio. We chose to use Mylar bags because they are inexpensive and initial testing of OPEnS using Mylar bags demonstrated that the combination of minimal open headspace and aluminum foil inner lining effectively constrained evaporative mass losses. Furthermore, they can be reused once properly cleaned and dried. The inside of the totalizer consists of a float chamber with a buoy. The buoy rises during rainfall events so that water can enter the collection bag, but otherwise sits over the spout to prevent contact between the water sample and the outside atmosphere.

Following initial field tests during which OPEnS totalizers developed stress cracks near the bag threads (section 2.2), the OPEnS totalizer was re-designed (version 2.0) using a more flexible resin material and UV-resistant paint. The narrow waist towards the bottom of the totalizer was filled in and the walls of the device around the top part of the bag threads were also made thicker (Fig. 1B). Small filets were added to the bag threads and the number of thread revolutions were reduced. The screw threads on the bottom of the totalizer were also adjusted for 22 mm spouts to accommodate the 3000-mL Mylar foil bags from IMPAK.

After additional field and laboratory tests (sections 2.2 and 2.3), the OPEnS totalizer was adjusted (version 3.0) to be free-standing so that it can operate independently without the METER station base, thus serving as a fully autonomous totalizing station (Fig. 1C). The inlet spout was removed from the top, and the cap was replaced with an 8.3 cm diameter funnel that drains through the float chamber into the 3000-mL collection bag. A stainless-steel mesh was added to the inside of the funnel to serve as a filter for large debris. A side-channel was included for 0.5 in rebar, to facilitate fixation of the totalizer to a stronger support. As a precaution against wind-induced instability, we added wire fencing around the entire totalizer extending below the bottom of the collection bag to help keep the bag in place and minimize stress on the bag threads due to wind. We also stuck adhesive pads onto the bag surfaces (Grainger 6EEE7). The pads have slots, which we used to thread in cable ties that kept them loosely in place against the support. A close-up and traverse and longitudinal cross section views of the OPEnS system are shown in Fig. 1D-F).

2.2. Field testing

OPEnS totalizers were installed alongside oil-based totalizers in April 2021 and operated through mid-2023 in the cities of San Antonio and Jolly, Texas, USA (Fig. 2). Both sites are classified as humid sub-tropical (Cfa) Köppen climates; however, according to Global Summary of the Month (GSOM) records from the National Centers for Environmental Information (NCEI) stations USW00012909 (~11 km SE of San Antonio) and USW00013966 (~15 km NW of Jolly), Jolly experienced a lower mean annual precipitation (MAP, 556 mm/y), lower mean annual temperature (MAT, 18.7 °C), and higher mean annual windspeed (MAW, 5.0 m/s) than San Antonio (MAP of 563 mm/y, MAT of 21.9 °C, and MAW of 3.5 m/s) during these years (NOAA NCEI, 2023).

In May 2021, after one month of operation, the OPEnS totalizer 1.0 in San Antonio began to swell along the bottom edge near the bag threads and by the following month began to crack. For this reason, no comparative samples were collected until December 2021 when gorilla tape was used to secure the bag to the totalizer. At this point, we regressed from using 3000-mL collection bags to using 1000-mL collection bags in conjunction with a 3785-mL (1 gal) High Density

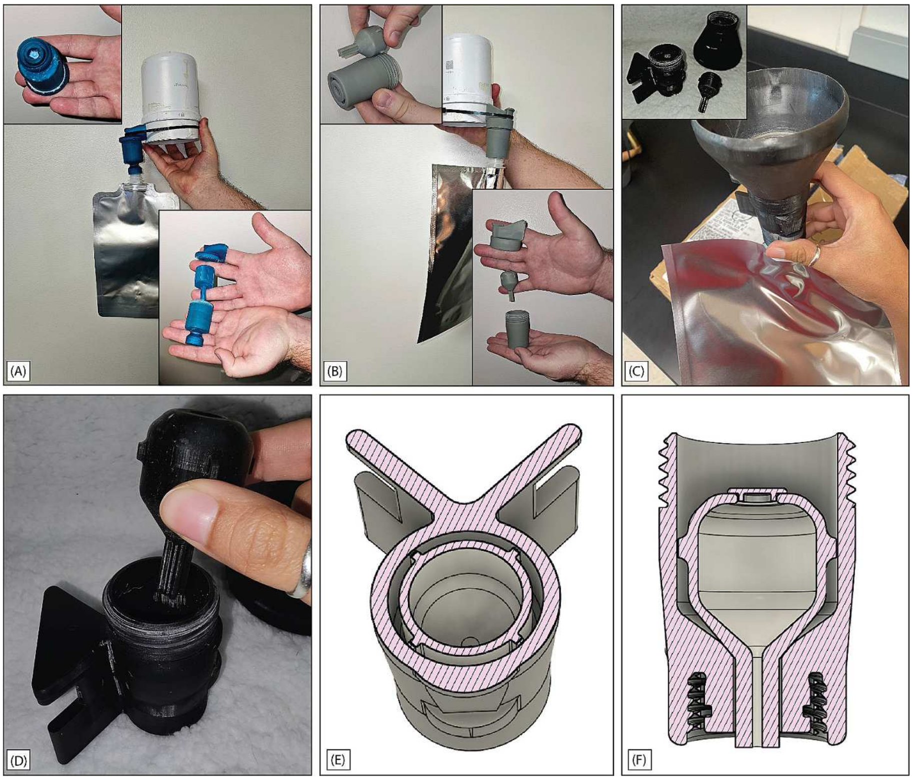

Fig. 1. Three versions of the OPEnS totalizer: versions 1 (A) and 2 (B) were designed as an attachment to METER's ATMOS 41 weather station, while version 3 (C) was designed to operate independently. All three versions consist of a cap (water route piece in versions 1 and 2, funnel piece in version 3), float, and float chamber with bag threads. A close-up (D) and traverse (E) and longitudinal (F) cross section views are shown.

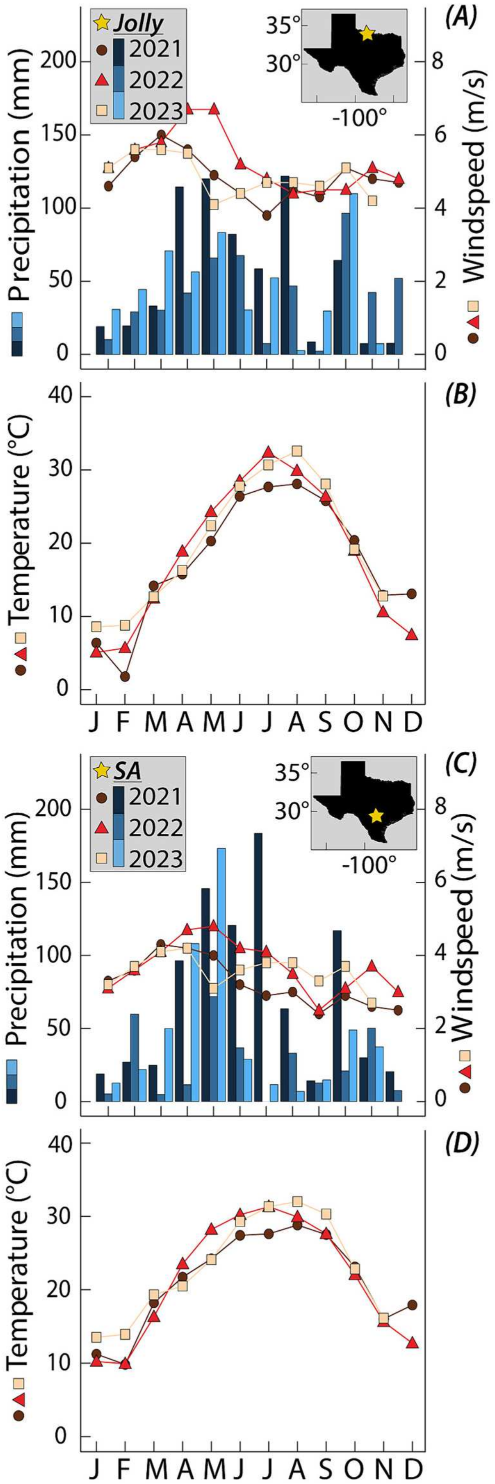

Fig. 2. Meteorological conditions during the sampling period, including the monthly precipitation totals and the average monthly windspeeds and temperatures, for testing sites Jolly in north-central Texas (A-B) and San Antonio in south-central Texas (C-D).

Polyethylene (HDPE) accumulation bottle (IAEA, 2014). The accumulation bottle was used to store rainfall from the collection bag, which was emptied into the accumulation bottle two or more times during a single month before the cumulative monthly sample was taken (a separate accumulation bottle was also used for the oil-based totalizer during wetter months). In August 2022, the OPEnS totalizer 2.0 was installed in San Antonio and this version was used to collect monthly samples with no further degradation issues through April 2023. In May 2023, the OPEnS totalizer 3.0 was installed and used without problem through August 2023.

In Jolly, the OPEnS totalizer 1.0 stayed intact from its initial installation in April 2021 through November 2021 (although we did start using 1000-mL bags with accumulation bottles in June due to the crack that developed early on along the OPEnS totalizer in San Antonio). In December 2021, the OPEnS totalizer in Jolly also began to crack, so no samples were collected until November 2022 when OPEnS 2.0 was installed in Jolly and was used to collect monthly samples through May 2023.

2.3. *Laboratory experiment*

Following Michelsen et al. (2018), we modified a laboratory oven to carry out a month-long (30 day) controlled experiment further testing the totalizers under extreme hot and dry conditions (Fig. S3). Every morning at 10:00 AM, the oven was set to heat up to 40 °C for 12 h then allowed to cool to ambient lab temperature overnight. Every other day, 600 g of fresh silica gel was placed into the oven's top shelf on a steel mesh tray to remove moisture. Zero air was continuously flushed at 2.5 psi (2 L/min) through a porous filter mat into the part of the oven containing the totalizers from a custom-made diffuser. The diffuser was assembled using Swagelok steel tubing that entered the oven through a port in the back wall of the oven and encircled the bottom floor. Four Swagelok union tees connected to the tubing were each centered along an oven wall, with their remaining open connections facing upwards to direct zero air through the filter mat. These remaining open connections were partially covered with Teflon tape to ensure that the flow of air being emitted by each tee was approximately equal. The steel tubing connecting all four tees ended in the middle of the oven and was left uncovered.

To ensure that a totalizer's position in our modified oven would not influence evaporation rate, we placed 56 25-mL beakers, each filled with 10 mL of water with a known isotopic composition (Houston DI; HDI), onto the bottom shelf of the oven at 40 °C for 48 h and compared their masses before and after oven exposure. Fig. S4B shows that our modified oven produces a more homogeneous evaporation pattern relative to the same oven unmodified (Fig. S4A), allowing for the placement of totalizers anywhere on the shelf except within ~5 cm of the oven's edge. To further ensure that oven position would not affect the experiment, the four totalizers were rotated clockwise each day after being weighed.

Three totalizers were tested: 1) OPEnS 2.0, 2) an oil-based totalizer, and 3) the commercially available tube dip-in totalizer (Palmex Ltd. RS1; Gröning et al., 2012). A fourth totalizer with no evaporation reduction mechanism was tested as a control. Each 3000-mL totalizer was filled to 12 % of its volume (360 mL) with HDI water and weighed once a day at 10 AM to determine evaporative mass losses. Samples were collected every three days using pipettes to track accompanying evaporative shifts. Samples were stored in 2 mL glass vials, capped, sealed with Parafilm, and stored in a refrigerator at 4 °C until analysis. The temperature and relative humidity of the oven and ambient lab were recorded every 5 min using HOBO U23 Pro V2 data loggers (Onset U23-001 A). We began the experiment on the 11th day of October 2022 (day 0) and collected the final totalizer masses and water samples on the 10th day of November 2022 (day 30).

2.4. *Isotopic analysis*

To remove potential organic matter contaminants, all samples were filtered (pore size 0.20 μm, VWR 28145–475), treated with granular activated carbon for 48 h, and filtered again. In some cases, samples from the oil-based totalizers were filtered a third time to eliminate remaining oil fractions.

Samples were analyzed for δD, $\delta^{18}O$, $\delta^{17}O$, and $\Delta'^{17}O$ in 2023 at the University of Houston (UH) using a Picarro L2140-i CRDS analyzer. Raw data were normalized to the VSMOW-SLAP scale using VSMOW2 ($\delta D = 0$ ‰, $\delta^{18}O = 0$ ‰, $\Delta'^{17}O = 0$ per meg) and SLAP2 ($\delta D = -427.50$ ‰, $\delta^{18}O = -55.50$ ‰, $\Delta'^{17}O = 0$ per meg) (Schoenemann et al., 2014). Additional standards KD (Kona deep ocean water), USGS45, and USGS46 were used for quality assurance/quality control (QA/QC). All standards used for data normalization and QA/QC were analyzed in sets according to the run architecture recommended by Schauer et al. (2016) (e.g., a conditioning vial followed by an analysis vial), and all standard and sample vials were injected 15 times but only the last 10 injections were used for data normalization to compensate for memory effects. Each analysis included three sets of SMOW and SLAP, two sets of KD, one or two sets of USGS45 and/or USGS46, and 20 to 36 samples.

Analytical precision was calculated using the pooled standard deviation (σ_p) of standard measurements as recommended for triple oxygen isotope samples by Aron et al. (2021):

$$\sigma_p = \sqrt{\frac{\sum_{i=1}^{k}(n_i - 1)s_i^2}{\sum_{i=1}^{k}(n_i - 1)}}$$

where s_i is the standard deviation, n_i is the number of replicate measurements of the i-th sample, and k is the total number of samples. Our long-term analytical precision was 0.5 ‰, 0.07 ‰, 0.04 ‰, and 5 per meg for δD, $\delta^{18}O$, $\delta^{17}O$, and $\Delta'^{17}O$, respectively, based on VSMOW ($n = 45$) and SLAP ($n = 41$). Our external precision was 0.3 ‰, 0.06 ‰, 0.04 ‰, and 9 per meg for δD, $\delta^{18}O$, $\delta^{17}O$, and $\Delta'^{17}O$, respectively, based on KD ($n = 30$), USGS45 ($n = 13$), and USGS46 ($n = 18$). A summary of our system's performance in 2023 is shown in Table S1. The final isotopic compositions that we present here for our samples are an average of corrected triplicate analysis (Tables S2, S3).

3. Results

3.1. Laboratory experiment

During our experiment, ambient lab temperature fluctuated between 20 and 22 °C with an average of 21.4 °C, and oven temperature varied from 23 to 40 °C with an average of 34.3 °C (Figs. S5 and S6). Relative humidity ranged from 21 to 53 % and 1 to 35 % in the lab and oven, respectively. Although the lab experienced an average relative humidity of 44 %, the oven maintained an average relative humidity of 9 % due to the silica gel and dry air. Maximum relative humidity peaks of >30 % at ~10:00 AM every morning are likely the result of: 1) opening the door to weigh the totalizers and 2) turning the oven back on to resume the experiment, causing any water that had condensed on oven surfaces during the cooler nighttime to evaporate. Relative humidity returned to <10 % within 30 min to 1 h after the oven was turned back on.

3.1.1. Evaporative water losses

The extreme simulated climate conditions resulted in considerable evaporation from all four tested totalizers. Table 1 shows the final mass losses measured from each totalizer in g (absolute values), % orig. (percentages of the original water mass of 360 mL), and % ref. (percentages normalized to the mass lost by the reference totalizer), and Table S4 shows their cumulative mass losses (in g) through time. By the end of the 30-day experiment, the OPEnS totalizer 2.0 had experienced the smallest mass loss of 0.74 g (0.21 % of its original mass and 12.78 % of the mass lost by the reference totalizer; Fig. 3). The oil-based totalizer lost 1.46 g (0.41 % of its original mass and 25.22 % of the mass lost by the reference totalizer), and the tube dip-in and reference totalizers exhibited much larger final mass losses of 4.95 (1.37 % of its original mass and 85.49 % of the mass lost by the reference totalizer) and 5.79 g (1.61 % of its original mass).

Table 1

The final (fin) evaporative mass losses (Δm), isotopic shifts ($\Delta\delta$), and deuterium (d) excess values after 30 days. The mass losses are expressed as absolute losses (g), as percentages of the original water mass (% orig.), and as percentages normalized to the reference collector (% ref.). The original d-excess was −0.6 ‰.

	OPEnS	Oil	Tube dip-in	Reference
Δm_{fin} (g)	0.74	1.46	4.95	5.79
Δm_{fin} (% orig.)	0.21	0.41	1.37	1.61
Δm_{fin} (% ref.)	12.78	25.22	85.49	100.00
$\Delta\delta D_{fin}$ (‰)	−0.9	0.3	0.8	2.1
$\Delta\delta^{18}O_{fin}$ (‰)	−0.04	0.16	0.23	0.83
d-excess$_{fin}$ (‰)	−1.1	−1.5	−1.6	−5.1

3.1.2. Isotopic shifts

Deviations from the original composition of HDI using each totalizer are shown in dual-isotope plots in Figs. 4 and 5 and are summarized in Table 1. The OPEnS totalizer 2.0 exhibited the smallest final shifts in δD, $\delta^{18}O$, and d-excess: −0.9 ‰, −0.04 ‰, and −0.5 ‰, respectively, remaining close to the isotopic composition of HDI. The water in the OPEnS totalizer 2.0 was never evaporatively enriched in δD and $\delta^{18}O$ beyond the values of external precision (0.3 and 0.06 ‰, respectively). The remaining totalizers showed systematic evaporative enrichment of δD and $\delta^{18}O$ through time. The oil-based totalizer became enriched beyond the 2σ external precision for $\delta^{18}O$ (0.6 ‰) between days 27 and 30, the tube dip-in totalizer between days 18 and 21, and the reference totalizer between days 3 and 6 (Table S2), with final $\delta^{18}O$ shifts of 0.16, 0.23, and 0.84 ‰, respectively. Wilcoxon rank sum tests indicate that the sample distribution medians of $\delta^{18}O$ and d-excess measurements are different for OPEnS 2.0 versus other totalizer types ($p < 0.05$; Table S5; see also Fig. 5). The d-excess of the water in the oil-based and tube dip-in totalizers was affected similarly by our extreme conditions with similar medians (Table S5) and final shifts of −0.9 and − 1.0 ‰, respectively, while the water in the reference totalizer showed a final d-excess shift of −4.5 ‰. Regarding $\Delta'^{17}O$, variations associated with all four totalizers stayed within the 2σ external precision (18 per meg) and technical performance guaranteed by Picarro (15 per meg) of the original value (−3 per meg) for the entire duration of the experiment.

3.2. Field testing

In Fig. 6, we present field data as differences between the isotopic compositions of samples collected using oil-based and OPEnS totalizers (e.g., δ_{oil} - δ_{OPEnS}) because the ranges of values for each site were found to be distinct (although measured values are also available in Table S3). Many monthly samples from San Antonio collected using OPEnS 1.0 and 2.0 were enriched with respect to δD and $\delta^{18}O$ relative their oil-based counterparts beyond the 2σ external precision (0.6 and 0.12 ‰, respectively), while most of those from Jolly showed similar δD and $\delta^{18}O$. Monthly samples collected from both sites using OPEnS 1.0 and 2.0 generally showed similar d-excess and $\Delta'^{17}O$ values as the oil-based totalizers except for those from two months in San Antonio. The mean δD, $\delta^{18}O$, d-excess, and $\Delta'^{17}O$ differences between monthly samples

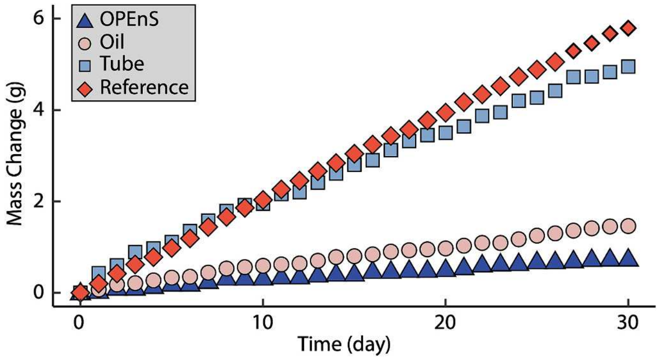

Fig. 3. The daily and cumulative evaporative mass losses associated with each totalizer.

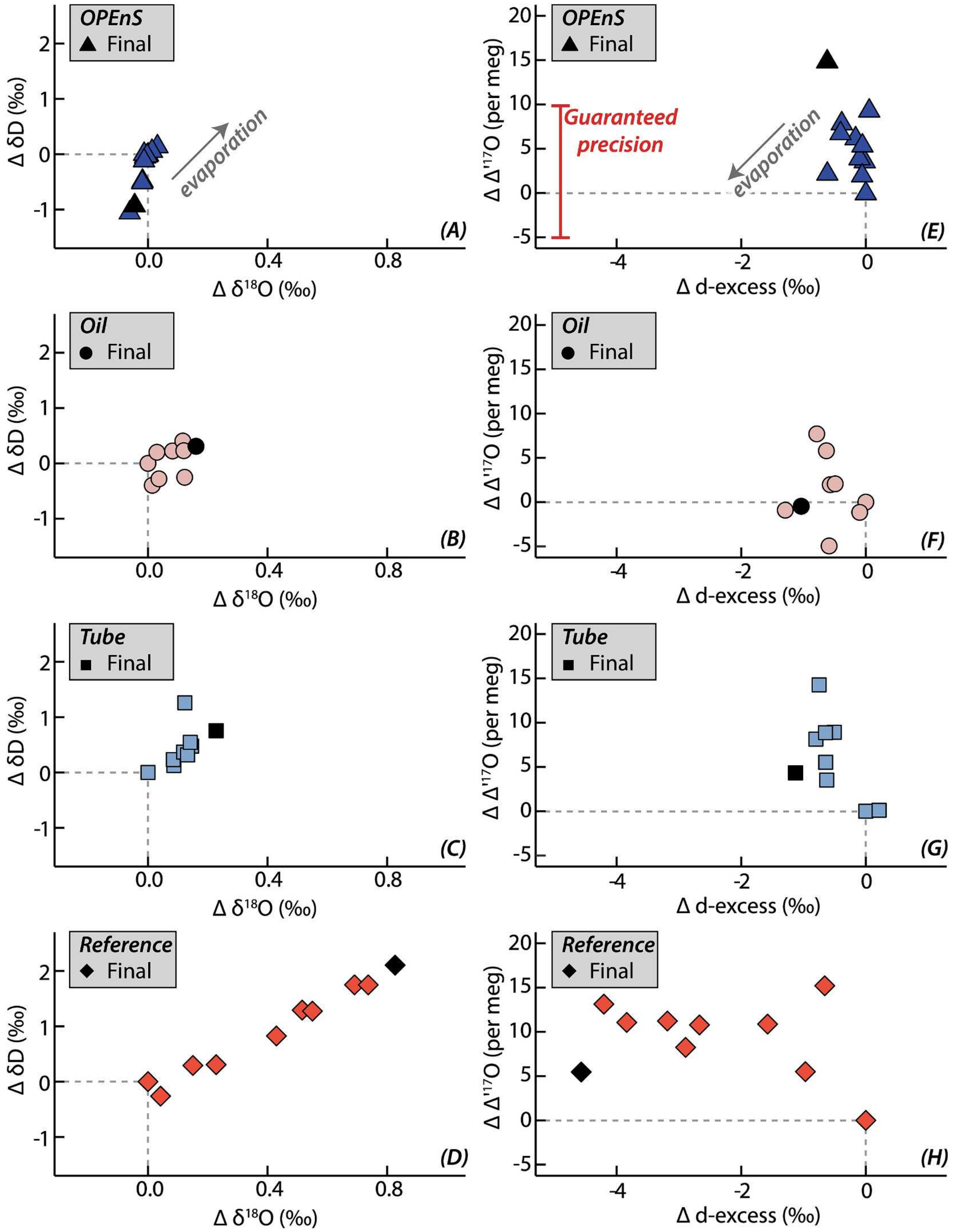

Fig. 4. The evaporative $\delta^{18}O$, δD, d-excess, and $\Delta'^{17}O$ shifts associated with each totalizer; dashed lines represent original values and black symbols represent final values.

improved from −3.3 ‰, −0.48 ‰, +0.5 ‰, and + 1 per meg, respectively, using OPEnS 1.0 to +0.4 ‰, +0.17 ‰, −1.0 ‰, and − 1 per meg, respectively, (within the 2σ external precision for all isotopic parameters) using OPEnS 3.0.

4. Discussion

4.1. Preservation of triple oxygen isotopes in rainfall totalizers

To date, many triple oxygen isotope studies have relied on opportunistic precipitation sampling, meteoric waters (rivers and/or lakes), or tap waters (Luz and Barkan, 2010; Li et al., 2015; Tian et al., 2020; Bershaw et al., 2020; Aron et al., 2021; Katz et al., 2023). These data types were a useful starting point; however, amount weighted monthly precipitation data are needed to refine our understanding of $\Delta'^{17}O$ variations through time (e.g., interseasonal, intraseasonal, and El Niño oscillations; He et al., 2021; Aron et al., 2021). The results of our 30-day controlled laboratory experiment suggest that the OPEnS, oil-based, and tube dip-in totalizers are likely capable of preserving the triple oxygen isotope compositions of monthly-integrated rainfall samples in most natural settings.

By the end of the 30 days, water from OPEnS 2.0 was still close to its original isotopic composition, while evaporation from the oil-based and tube dip-in totalizers had produced large δD and $\delta^{18}O$ shifts that are

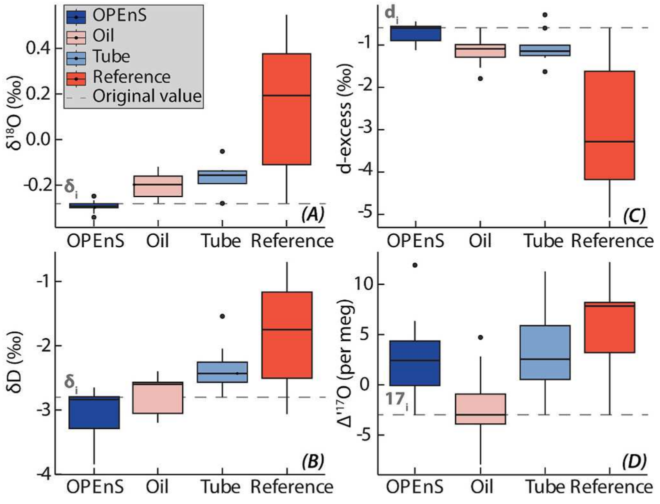

Fig. 5. Boxplots showing the distributions and mean values of δ^{18}O, δD, d-excess, and Δ'^{17}O; outliers are shown as black circles, and dashed lines represent original values.

comparable to those reported in the original 32-day experiment using the same totalizers by Michelsen et al. (2018). The main difference between the two experiments is that we selected a slightly lower filling volume to exacerbate any potential evaporative effects on Δ'^{17}O; still, samples from the OPEnS 2.0, oil-based, and tube dip-in totalizers all stayed within the 2σ external precision and guaranteed precision for Δ'^{17}O. The conditions simulated in our laboratory experiment are characteristic of hot arid Köppen climates (BWh), which characterize places like Death Valley, California (USA) and parts of the Sahara Desert of northern Africa (Hunt, 1966). Therefore, our experiment represents the most extreme evaporative conditions possible on earth, and the performance of oil-based and tube dip-in totalizers in terms of δD and δ^{18}O preservation would be improved in less harsh settings. For example, over one year in Vienna, Gröning et al. (2012) measured δD and δ^{18}O shifts of only 1.3 and 0.08 ‰, respectively, using the tube dip-in totalizer. We recommend that before implementing any type of rainfall totalizer researchers conduct tests under the expected environmental conditions for their study area, either in a laboratory setting or using a field control (e.g., an additional covered/rain-protected totalizer filled with water of a known isotopic composition used to evaluate isotopic integrity post-sample collection; Scholl et al., 1996, 2011).

4.2. *Comparison of conventional and OPEnS rainfall totalizers*

After a few design modifications, the OPEnS 2.0 totalizer outperformed the oil-based totalizer in both the lab experiment and field deployment in Jolly. The cracks that developed along OPEnS 1.0 at both field sites were likely the result of shrinking and swelling due to temperature and moisture fluctuations. The strength, elasticity, and other mechanical properties of photopolymers (light-activated resin used in 3D printing), especially the semi-transparent varieties such as the one used to print OPEnS 1.0, are vulnerable to degradation when exposed to heat, light, or oxygen (Yousif and Haddad, 2013). Isotopic discrepancies between monthly samples collected from the OPEnS 1.0 and oil-based totalizers were high (Fig. 6), so the OPEnS totalizers 2.0 and 3.0 were designed with a more flexible resin and UV-resistant coat.

In addition, the original OPEnS totalizer 1.0 was not ideal for monthly collection at locations with intense rainfall because it was not designed to collect >250 mL of water and was at risk of tearing at the bag threads or overflowing and losing all or part of the cumulative sample during such periods. Therefore, structural changes to OPEnS 2.0 and 3.0 were made to reduce stress concentration and thread failure for bags up to 3000-mL. After the redesign, we experienced no further issues with cracking, tearing, or overflowing using OPEnS 2.0 or 3.0 at either field site, and isotopic data show close agreement with conventional oil-based totalizers (Fig. 6).

To gain further insight into the isotopic differences between the OPEnS 2.0 and oil-based totalizers, we considered the climate parameters at each field site. There are weak correlations between the differences in monthly δ^{18}O values of the oil-based and OPEnS 2.0 totalizers ($\delta^{18}O_{oil}$ - $\delta^{18}O_{OPEnS2.0}$) and: 1) windspeed, 2) precipitation amount, and 3) temperature in Jolly ($R^2 = 0.25$, 0.16, and 0.25, respectively), with higher windspeeds, lower precipitation amounts, and cooler temperatures relating to more enriched OPEnS samples relative to oil samples. The $\delta^{18}O_{oil}$ and $\delta^{18}O_{OPEnS2.0}$ differences do not correlate with windspeed or precipitation amount in San Antonio; this could be because this site has lower monthly windspeeds and higher monthly precipitation amounts (Fig. 2). High monthly precipitation amounts may buffer evaporative effects (Leng and Marshall, 2004; Liu et al., 2018). Despite the potential environmental influences on OPEnS 2.0, the average $\delta^{18}O_{oil}$ - $\delta^{18}O_{OPEnS2.0}$ difference was smaller than the 2σ external precision in Jolly. Furthermore, the δD, δ^{18}O, and Δ'^{17}O oil – OPEnS 3.0 differences are all within the 2σ external precision over four months of preliminary testing in San Antonio. Further testing of OPEnS 3.0 is in progress, and files for previous versions and the final, validated version will be available on the OPEnS lab GitHub (https://github.com/OPEnSLab-OSU/OPEnS-Lab-Home/wiki).

4.3. *Outlook and advantages of the OPEnS system*

With this laboratory and field testing that provides proof of concept of the OPEnS system, future studies can continue to improve the design with relative simplicity due to the open accessibility of the files. An added benefit of the system is that it is fully customizable to a project's needs. Both the funnel and bag size can be adjusted for small or large volumes of rainfall or short or long sampling time periods. This will allow the gas/water ratio inside of the collection bag of the totalizer itself to remain low compared to that inside of totalizers employing collection bottles (although caution should still be applied if using an accumulation bottle with the OPEnS system, to select a bottle size that will not be conducive to in-bottle evaporative losses during the sampling period; IAEA, 2014). OPEnS is intended to be applicable for both small and large-scale projects and many universities now have 3-D printers available, allowing for wide applicability of this method. While large-scale injection modeling could produce stronger parts with more durable materials than those available for 3D printing (such as HDPE), it involves higher costs and less flexibility for customized production. Oil or tube dip-in totalizers demand more invasive modifications in areas with very low monthly precipitation amounts (Gröning et al., 2012; Michelsen et al., 2018). For example, Gröning et al. (2012) suggest shortening the inner tube of the tube dip-in totalizer and adding a small bucket inside the collection bottle for the tube to dip into so that even a small amount of rain would immerse the end of the tube and seal the headspace off from atmospheric contact.

Another advantage of OPEnS system is that sample preparation requires little time and effort and can be easily performed without the need for separatory funnels or other specialized tools used in oil removal (summarized in Michelsen et al., 2018), simplifying collections for both researchers and citizen scientists who often help with these types of projects. Totalizer maintenance is also straightforward; it only requires a few minutes to change out the collection bag and clean and dry the funnel and float chamber in-between sampling periods. Oil-based totalizers must include at least ~5 mm of oil to prevent evaporation (IAEA, 2014), but Weaver and Talma (2007) recommend 20 mm in extremely hot, dry conditions. However, we found that when the monthly precipitation amount is low relative to the oil amount, it can be particularly difficult to separate the oil from the water sample for analysis, creating the potential for oil contamination in analyses and requiring significant maintenance of IRMS or laser spectroscopy systems. These qualities of

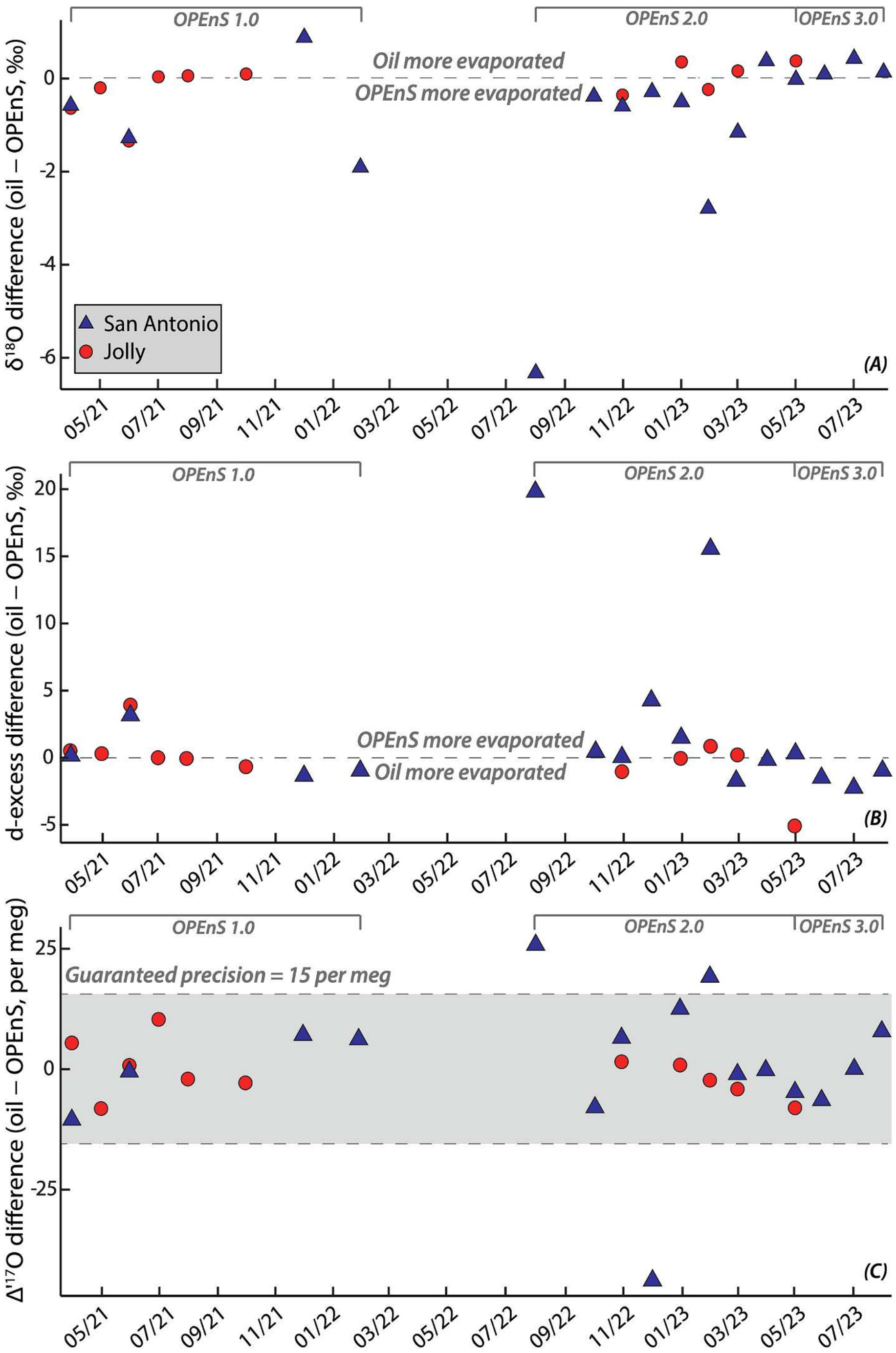

Fig. 6. Field test results, where data are shown as differences between the $\delta^{18}O$ (A), d-excess (B), and $\Delta'^{17}O$ (C) of samples collected using oil-based and OPEnS totalizers.

OPEnS distinguish it from traditional oil and tube totalizers, and the results presented in this study are promising.

Future testing could also test for factors such as windspeed and precipitation amount that were not incorporated into our controlled experiment and may affect the performance of OPEnS totalizers in the field. Under-catch, where accelerated wind causes increased turbulence above a rain gauge resulting in the deflection of falling raindrops away from the collection orifice, is a common issue in rainfall collection (WMO, 2008). Gauges with inverted conical shapes and large semi-vertical angles (e.g., funnels) are more aerodynamic and show improved catch efficiencies compared to conventional cylinder-shaped gauges with straight edges (Strangeways, 2004; Colli et al., 2018; Pollock et al., 2018). The OPEnS totalizers 1.0 and 2.0 used the cylindrical METER rain gauge, while the most recent OPEnS totalizer 3.0 replaces the METER base with a funnel that should help minimize under-catch in future implementations (Fig. 1).

5. Conclusions

In this study, we carried out a controlled lab experiment to evaluate three rainfall totalizers (OPEnS, tube dip-in, and oil) for their potential application to triple oxygen isotope studies of monthly precipitation. In the laboratory, we simulated a 23 to 40 °C diurnal temperature regime and 9.1 % average relative humidity to test the totalizers under extreme evaporative conditions. The OPEnS totalizer, designed to be compatible with the METER ATMOS 41 weather station, showed the smallest evaporative mass losses and δD, δ^{18}O, and d-excess shifts, and its Δ'^{17}O values were within external precision of the original value. OPEnS also has the advantage of being oil-free, requiring less effort during sample collection and preparation and presenting less risk of machine contamination during analysis (Prechsl et al., 2014; Hartmann et al., 2018). Furthermore, since the collection bags used by the OPEnS totalizer expand as they fill there is minimal headspace, so the gas/water ratio inside of the OPEnS totalizer remains low relative to the tube dip-in totalizer, which has exhibited considerable in-bottle evaporative losses in arid climates (Crawford et al., 2017). Although the well-established oil-based and tube dip-in methods resulted in measurable δD, δ^{18}O, and d-excess shifts by the end of our lab experiment, we anticipate that their performance would be acceptable in more temperate environments, especially because their Δ'^{17}O values were within external precision of the original value.

We further tested OPEnS totalizers against oil-based totalizers in a field setting at two sites in the towns of Jolly and San Antonio, Texas. Although the original OPEnS 1.0 failed due to material and structural issues, OPEnS 2.0 and 3.0 performed on par with the oil-based totalizer. OPEnS 3.0 is more aerodynamic to reduce wind effects on rainfall collection and can be implemented independently from the METER ATMOS 41 thus allowing for rescaling of the funnel component according to different expected precipitation amounts and/or sampling time-periods. Longer field tests of OPEnS 3.0 under a variety of environmental conditions are ongoing, including tests involving smaller funnel and/or larger bag components for those regions subject to intense storms. However, our initial laboratory experiment and field tests in Texas indicate that the OPEnS method performs similarly or better than conventional rainfall totalizers designed to prevent secondary evaporation for isotopic monitoring.

CRediT authorship contribution statement

L. Nicole Arellano: Writing – original draft, Visualization, Methodology, Investigation, Formal analysis, Data curation, Conceptualization. **Emily J. Beverly:** Writing – review & editing, Validation, Supervision, Resources. **John S. Selker:** Writing – review & editing, Resources, Methodology, Investigation, Funding acquisition, Conceptualization. **Mitchell Nelke:** Methodology, Investigation, Conceptualization. **Gurpreet Singh:** Methodology, Investigation. **Cara Walter:** Methodology, Investigation.

Declaration of competing interest

The authors declare that they have no known competing financial interests or personal relationships that could have appeared to influence the work reported in this paper.

Data availability

Data will be made available on request.

Acknowledgments

The authors would like to thank Gilbert and Melissa Rodriguez for their help collecting monthly precipitation samples at Jolly and San Antonio.

Appendix A. Supplementary data

Supplementary data to this article can be found online at https://doi.org/10.1016/j.chemgeo.2024.122351.

References

Angert, A., Cappa, C., Depaolo, D., 2004. Kinetic 17O effects in the hydrologic cycle: indirect evidence and implications. Geochim. Cosmochim. Acta 68, 3487–3495.

Aron, P., Levin, N., Beverly, E., Huth, T., Passey, B., Pelletier, E., Poulsen, C., Winkelstern, I., Yarian, D., 2021. Triple oxygen isotopes in the water cycle. Chem. Geol. 565, 120026.

Barkan, E., Luz, B., 2005. High precision measurements of 17O/16O and 18O/16O ratios in H2O. Rapid Commun. Mass Spectrom. 19, 3737–3742.

Barkan, E., Luz, B., 2007. Diffusivity fractionations of $H_2^{16}O/H_2^{17}O$ and $H_2^{16}O/H_2^{18}O$ in air and their implications for isotope hydrology. Rapid Commun. Mass Spectrom. 21, 2999–3005.

Bershaw, J., Hansen, D.D., Schauer, A.J., 2020. Deuterium excess and 17O-excess variability in meteoric water across the Pacific Northwest, USA. Tellus Ser. B Chem. Phys. Meteorol. 72, 1–17.

Cao, X., Liu, Y., 2011. Equilibrium mass-dependent fractionation relationships for triple oxygen isotopes. Geochim. Cosmochim. Acta 75, 7435–7445.

Colli, M., Pollock, M., Stagnaro, M., Lanza, L.G., Dutton, M., O'Connell, E., 2018. A Computational Fluid-Dynamics Assessment of the improved Performance of Aerodynamic rain Gauges. Water Resour. Res. 54, 779–796.

Craig, H., 1961. Isotopic Variations in Meteoric Waters. Science 133, 1702–1703.

Crawford, J., Hollins, S.E., Meredith, K.T., Hughes, C.E., 2017. Precipitation stable isotope variability and subcloud evaporation processes in a semi-arid region. Hydrol. Process. 31, 20–34.

Dansgaard, W., 1964. Stable isotopes in precipitation. Tellus 16, 436–468.

Fischer, B.M.C., Aemisegger, F., Graf, P., Sodemann, H., Seibert, J., 2019. Assessing the Sampling Quality of a Low-Tech Low-Budget Volume-based Rainfall Sampler for Stable Isotope Analysis. Front. Earth Sci. 7, 244.

Gröning, M., Lutz, H., Roller-Lutz, Z., Kralik, M., Gourcy, L., Poltenstein, L., 2012. A simple rain collector preventing water re-evaporation dedicated for delta O-18 and delta H-2 analysis of cumulative precipitation samples.

Hartmann, A., Luetscher, M., Wachter, R., Holz, P., Eiche, E., Neumann, T.A., 2018. Technical note: GUARD@_ An automated fluid sampler preventing sample alteration by contamination, evaporation and gas exchange, suitable for remote areas and harsh conditions. Hydrol. Earth Syst. Sci. 22, 4281–4293.

He, S., Jackisch, D., Samanta, D., Yi, P.K.Y., Liu, G., Wang, X., Goodkin, N.F., 2021. Understanding Tropical Convection through Triple Oxygen Isotopes of Precipitation from the Maritime Continent. J. Geophys. Res. Atmos. 126 e2020JD033418.

Hunt, C.B., 1966. Hydrologic Basin, Death Valley. California, US Government Printing Office.

IAEA (2014) IAEA/GNIP precipitation sampling guide Introduction: the Global Network of Isotopes in Precipitation (GNIP).

IAEA and WMO, 2018. Global Network of Isotopes in Precipitation (The GNIP Database).

Kaseke, K.F., Wang, L., Wanke, H., Tian, C., Lanning, M., Jiao, W., 2018. Precipitation origins and key drivers of precipitation isotope (18 O, 2 H, 17 O) compositions over Windhoek. J. Geophys. Res. Atmos. 123.

Katz, S.A., Levin, N.E., Rodbell, D.T., Gillikin, D.P., Aron, P.G., Passey, B.H., Tapia, P.M., Serrepe, A.R., Abbott, M.B., 2023. Detecting hydrologic distinctions among Andean lakes using clumped and triple oxygen isotopes. Earth Planet. Sci. Lett. 602, 117927.

Kralik, M., Papesch, W., Stichler, W., 2004. Austrian Network of Isotopes in Precipitation (ANIP): Quality assurance and climatological phenomenon in one of the oldest and densest networks in the world. International Atomic Energy Agency (IAEA).

Leng, M., Marshall, J., 2004. Palaeoclimate interpretation of stable isotope data from lake sediment archives. Quat. Sci. Rev. 23, 811–831.

Li, S., Levin, N.E., Chesson, L.A., 2015. Continental scale variation in 17O-excess of meteoric waters in the United States. Geochim. Cosmochim. Acta 164, 110–126.

Liu, W., Zhang, P., Zhao, C., Wang, H., An, Z., Liu, H., 2018. Reevaluation of carbonate concentration and oxygen isotope records from Lake Qinghai, the northeastern Tibetan Plateau. Quat. Int. 482, 122–130.

Luz, B., Barkan, E., 2010. Variations of 17O/16O and 18O/16O in meteoric waters. Geochim. Cosmochim. Acta 74, 6276–6286.

Majoube, M., 1971. Fractionnement en oxygène 18 et en deutérium entre l'eau et sa vapeur. J. Chim. Phys. 68, 1423–1436.

Michelsen, N., van Geldern, R., Roßmann, Y., Bauer, I., Schulz, S., Barth, J., Schüth, C., 2018. Comparison of Precipitation Collectors Used in Isotope Hydrology. Chem. Geol, p. 488.

NOAA NCEI, 2023. Climate Data Online Search. Glob. Summ. Mon.

Pollock, M.D., O'Donnell, G., Quinn, P., Dutton, M., Black, A., Wilkinson, M.E., Colli, M., Stagnaro, M., Lanza, L.G., Lewis, E., Kilsby, C.G., O'Connell, P.E., 2018. Quantifying and Mitigating Wind-Induced Undercatch in Rainfall Measurements. Water Resour. Res. 54, 3863–3875.

Prechsl, U.E., Gilgen, A.K., Kahmen, A., Buchmann, N., 2014. Reliability and quality of water isotope data collected with a low-budget rain collector. Rapid Commun. Mass Spectrom. 28, 879–885.

Risi, C., Bony, S., Vimeux, F., Chong, M., Descroix, L., 2010. Evolution of the stable water isotopic composition of the rain sampled along Sahelian squall lines. Q. J. R. Meteorol. Soc. 136, 227–242.

Sánchez-Murillo, R., Esquivel-Hernández, G., Sáenz-Rosales, O., Piedra-Marín, G., Fonseca-Sánchez, A., Madrigal-Solís, H., Ulloa-Chaverri, F., Rojas-Jiménez, L.D., Vargas-Víquez, J.A., 2017. Isotopic composition in precipitation and groundwater in the northern mountainous region of the Central Valley of Costa Rica. Isot. Environ. Health Stud. 53, 1–17.

Sánchez-Murillo, R., Durán-Quesada, A.M., Esquivel-Hernández, G., Rojas-Cantillano, D., Birkel, C., Welsh, K., Sánchez-Llull, M., Alonso-Hernández, C.M., Tetzlaff, D., Soulsby, C., Boll, J., Kurita, N., Cobb, K.M., 2019. Deciphering key processes controlling rainfall isotopic variability during extreme tropical cyclones. Nat. Commun. 10, 1–10.

Schauer, A.J., Schoenemann, S.W., Steig, E.J., 2016. Routine high-precision analysis of triple water-isotope ratios using cavity ring-down spectroscopy. Rapid Commun. Mass Spectrom. 30, 2059–2069.

Scholl, M.A., Ingebritsen, S.E., Janik, C.J., Kauahikaua, J.P., 1996. Use of Precipitation and Groundwater Isotopes to Interpret Regional Hydrology on a Tropical Volcanic Island: Kilauea Volcano Area, Hawaii. Water Resour. Res. 32, 3525–3537.

Scholl, M., Eugster, W., Burkard, R., 2011. Understanding the role of fog in forest hydrology: stable isotopes as tools for determining input and partitioning of cloud water in montane forests. Hydrol. Process. 25, 353–366.

Schürch, M., Kozel, R., Schotterer, U., Tripet, J.-P., 2003. Observation of Isotopes in the Water Cycle – the Swiss National Network (NISOT). Environ. Geol. 45, 1–11.

Sevruk, B., Ondrás, M., Chvíla, B., 2009. The WMO precipitation measurement intercomparisons. Atmos. Res. 92, 376–380.

Steig, E., Gkinis, V., Schauer, A., Schoenemann, S., Samek, K., Hoffnagle, J., Dennis, K., Tan, S., 2014. Calibrated high-precision 17Oexcess measurements using laser-current tuned cavity ring-down spectroscopy. Atmos. Meas. Tech. Discuss. 6, 10191–10229.

Strangeways, I., 2004. Improving precipitation measurement. Int. J. Climatol. 24, 1443–1460.

Stumpp, C., Klaus, J., Stichler, W., 2014. Analysis of long-term stable isotopic composition in German precipitation. J. Hydrol. 517, 351–361.

Sun, C., Tian, L., Shanahan, T.M., Partin, J.W., Gao, Y., Piatrunia, N., Banner, J., 2022. Isotopic variability in tropical cyclone precipitation is controlled by Rayleigh distillation and cloud microphysics. Commun. Earth Environ. 3, 50.

Tian, C., Wang, L., Jiao, W., Li, F., Tian, F., Zhao, S., 2020. (2019) Triple isotope variations of monthly tap water in China. Sci. Data 71 (7), 1–6.

Vreča, P., Malenšek, Andolšek N., 2016. Slovenian Network of Isotopes in Precipitation (SLONIP) – a review of activities in the period 1981–2015. Geologija 59, 67–84.

Wang, S., Zhang, M., Hughes, C.E., Zhu, X., Dong, L., Ren, Z., Chen, F., 2016. Factors controlling stable isotope composition of precipitation in arid conditions: an observation network in the Tianshan Mountains, Central Asia. Tellus Ser. B Chem. Phys. Meteorol. 68, 26206–26214.

Weaver, J.M.C., Talma, A.S., 2007. Cumulative rainfall collectors – a tool for assessing groundwater recharge. Water SA 31, 283–290.

WMO, 2008. Guide to hydrological practices.

Yousif, E., Haddad, R., 2013. Photodegradation and photostabilization of polymers, especially polystyrene: Review. Springerplus 2.

Zhu, G., Zhang, Z., Guo, H., Zhang, Y., Yong, L., Wan, Q., Sun, Z., Ma, H., 2021. Below-Cloud Evaporation of Precipitation Isotopes over Mountains, oases, and Deserts in Arid areas. J. Hydrometeorol. 22, 2533–2545.